Fluctuating Forces Induced by Non Equilibrium and Coherent Light Flow

Ariane Soret[1,2], Karyn Le Hur[2], Eric Akkermans[1*]
[1] *Department of Physics, Technion – Israel Institute of Technology, Haifa 3200003, Israel and*
[2] *Centre de Physique Théorique, École Polytechnique,*
CNRS, Université Paris-Saclay, 91128 Palaiseau, France

We show that mesoscopic coherent fluctuations of light propagating in random media induce fluctuating radiation forces. A hydrodynamic Langevin approach is used to describe the coherent light fluctuations, whose noise term accounts for mesoscopic coherent effects. This description – generalizable to other quantum or classical wave problems – allows to understand coherent fluctuations as a non equilibrium light flow, characterized by the diffusion coefficient D and the mobility σ, otherwise related by a Einstein relation. The strength of these fluctuating forces is determined by a single dimensionless and tunable parameter, the conductance $g_{\mathcal{L}}$. Orders of magnitude of these fluctuation forces are offered which show experimental feasibility.

Casimir physics covers a wealth of phenomena where forces between macroscopic objects are induced by long range fluctuations [1] of either classical or quantum origin. Fluctuations of the quantum electrodynamic (QED) vacuum epitomize this type of physics [2], but such fluctuation induced forces (FIF) arise in a wide range of systems [3–7].

In weakly disordered media, light intensity has long ranged spatial fluctuations (speckle) associated to mesoscopic coherent effects resulting from elastic multiple scattering. Here, we show that, unexpectedly, these intensity fluctuations lead to measurable FIF, $\boldsymbol{f} = \mathbf{f} - \langle \mathbf{f} \rangle$ (see Fig.1), on top of the disorder averaged radiation forces $\langle \mathbf{f} \rangle$.

The amplitude of the fluctuating radiation forces is

$$\langle \boldsymbol{f}^2 \rangle = \frac{1}{g_{\mathcal{L}}} \frac{\mathcal{P}^2}{v^2} \left(\mathcal{Q}_2 + \mathcal{Q}_\nu \right) . \tag{1}$$

This rather simple expression constitutes a central result of this work. It states that the fluctuating forces induced by coherent mesoscopic effects, besides their dependence upon the power $\mathcal{P}$ of the incoming light beam and the group velocity v, are driven by the dimensionless parameter $g_{\mathcal{L}}$ which encapsulates both the geometry and the scattering properties of the random medium. It is the analog of conductance in electronic systems, henceforth called conductance. The two dimensionless numbers $\mathcal{Q}_2$ and $\mathcal{Q}_\nu$ depend on the shape of the system and on boundary conditions but not on its volume nor on scattering properties. These different quantities are detailed in the sequel.

Quite remarkably, spatially coherent light fluctuations can be thoroughly described using a Langevin equation, where a properly tailored noise accounts for mesoscopic coherent effects. This non intuitive result proves effective to establish Eq.(1). Moreover, this approach is of particular interest since it maps the problem of coherent multiple light scattering onto an effective non equilibrium light flow characterized by two parameters only, the diffusion coefficient D and the strength of the noise σ, otherwise related by a Einstein relation. The scarcity of measurable and temperature independent non equilibrium phenomena makes the present proposal particularly relevant to experimental inspections. Indeed, since light induced fluctuating forces depend on the easily tunable parameter $g_{\mathcal{L}}$, coherent multiple light scattering offers setups where FIF are significantly enhanced compared to other known situations [8–13].

Consider a random and d-dimensional dielectric medium of volume $V = L^d$, illuminated by a monochromatic, scalar radiation [14], of wave-number k, incident along the direction of unit vector $\widehat{\mathbf{k}}$ (see Fig.1.a). Inside the medium, the amplitude $E(\mathbf{r})$ of the radiation is solution of the scalar Helmholtz equation,

$$\Delta E(\mathbf{r}) + k^2 \left(1 + \mu(\mathbf{r})\right) E(\mathbf{r}) = s_0(\mathbf{r}) \, , \tag{2}$$

where $\mu(\mathbf{r}) = \delta\epsilon(\mathbf{r})/\langle \epsilon \rangle$ denotes the fluctuation of the dielectric constant $\epsilon(\mathbf{r}) = \langle \epsilon \rangle + \delta\epsilon(\mathbf{r})$, $\langle \cdots \rangle$ is the average over disorder realizations and $s_0(\mathbf{r})$ is the source of the radiation. Disorder averaging allows to characterise the radiation propagation in the medium by the elastic mean free path l.

Multiple scattering solutions of the Helmholtz equation (2) are notoriously difficult to obtain. In the weak disorder limit $kl \gg 1$, an equivalent description of the local radiation at a point $\mathbf{r}$ and propagating along a direction $\widehat{\mathbf{s}}$ is provided by the specific intensity $I(\mathbf{r}, \widehat{\mathbf{s}})$, and the light current $\mathbf{j}(\mathbf{r}) = v\overline{I(\mathbf{r}, \widehat{\mathbf{s}})\, \widehat{\mathbf{s}}}$ averaged over all directions $\widehat{\mathbf{s}}$ [15, 16] (see SM section 1.2). In this approach, the force exerted by light on an absorbing surface S of normal vector $\widehat{\mathbf{n}}$, immersed inside the scattering medium, Fig.1.a, is

$$\mathbf{f} = \frac{\widehat{\mathbf{n}}}{v^2} \int_S d\mathbf{r} \; \mathbf{j}(\mathbf{r}) \cdot \widehat{\mathbf{n}} \; . \tag{3}$$

A Fick's law of diffusion coefficient $D = vl/d$,

$$\mathbf{j_D}(\mathbf{r}) = -D \boldsymbol{\nabla} I_D(\mathbf{r}) \, , \tag{4}$$

relates the disorder averaged light current $\mathbf{j_D}(\mathbf{r})$ to the disorder and direction averaged intensity $I_D(\mathbf{r})$. The latter obeys a diffusion equation, whose solutions have the

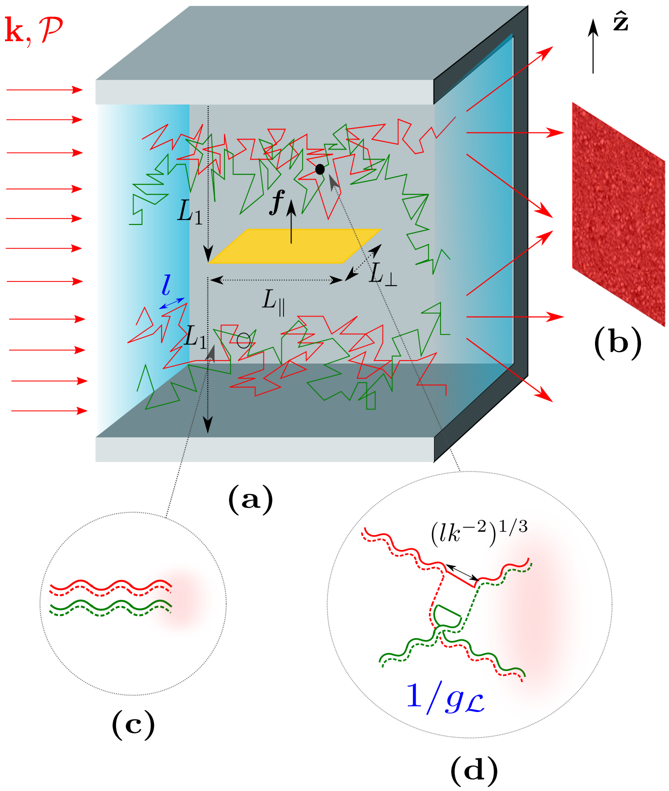

FIG. 1. **(a)** A monochromatic light beam of wave-number k and power $\mathcal{P}$ experiences multiple elastic scattering in a random dielectric medium. For weak disorder, $kl \gg 1$, the average diffusive light intensity $I_D(\mathbf{r})$ is represented by brownian-like trajectories. **(b)** For each disorder realization, speckle patterns of bright and dark spots evidence spatial fluctuations of light intensity whose correlations are due to interference processes illustrated in **(c)** and **(d)**. **(c)** Two phase-independent diffusive trajectories are built out of paired multiple scattering amplitudes – solution of Eq.(2) – having opposite phases and pictured by two coupled (full and dotted) wave-shaped lines. These independent diffusive paths contribute to short range correlations. **(d)** Coherent long ranged correlations result from quantum crossings and a new pairing of phase-dependent amplitudes between two diffusive trajectories. The occurrence of a quantum crossing is proportional to $1/g_{\mathcal{L}}$ (see text). Coherent light fluctuations induce a fluctuating force $\boldsymbol{f}$ on a (suspended) plate immersed inside the scattering medium. When placed at equal distance L_1 from the lower and upper box edges, the average radiation force on both sides of the plate cancels out, leaving only the finite fluctuating part $\boldsymbol{f}$.

generic form

$$I_D(\mathbf{r}) = \frac{v\mathcal{P}}{DL}\, h(\mathbf{r}) \tag{5}$$

where $h(\mathbf{r})$ is a dimensionless function determined by the geometry and boundary conditions and L is a typical geometric size of the medium (see SM section 1.2). Inserting Eq.(4) into Eq.(3) allows to obtain the average radiation force $\langle \mathbf{f} \rangle$. Its value, for an incident light beam perpendicular to a surface placed inside the medium at a distance L from the incidence plane, is $\langle \mathbf{f} \rangle = \mathcal{P}T(L)/v$, where T is the transmission coefficient (see SM section 2).

All phase dependent effects, responsible for speckle patterns (Fig.1.b), have been washed out in the disorder average diffusive limit underlying Eq.(4). A well defined semi-classical description enables to include coherent effects in a systematic way. It starts by noting (see Fig.1.c) that each diffusive trajectory is built from the pairing of two identical but time reversed multiple scattering amplitudes obtained from scattering solutions of Eq.(2). By construction, these two amplitudes have opposite phases so that the resulting diffusive trajectory is phase independent. Unpairing these two sequences gives access to the underlying phase carried by each multiple scattering amplitude and thereby to phase coherent corrections. The aforementioned description makes profit of this remark to evaluate phase coherent corrections (see Fig.1.d). At a local crossing, two diffusive trajectories mutually exchange their phase so as to form two new phase independent diffusive trajectories. This local crossing – or quantum crossing – is a phase dependent correction propagated over long distances by means of diffusive trajectories [17]. The occurrence of a quantum crossing (Fig.1.d), in a disordered medium of volume L^d is solely controlled by the conductance $g_{\mathcal{L}}$, a dimensionless parameter which depends on scattering properties and on the geometry of the medium. From now on and without loosing in generality, we consider the three dimensional ($d = 3$) setup displayed in Fig.1. The conductance $g_{\mathcal{L}}$ is then of the form

$$g_{\mathcal{L}} \equiv \frac{k^2 l}{3\pi}\mathcal{L} \tag{6}$$

where the length $\mathcal{L}$ depends on the geometry (see later and SM section 5.2 for examples) [18]. In the weak disorder limit $kl \gg 1$, the conductance $g_{\mathcal{L}} \gg 1$ and small coherent corrections generated by quantum crossings show up as powers of $1/g_{\mathcal{L}}$. This scheme allows to expand spatial correlations of the fluctuating light intensity $\delta I(\mathbf{r}) \equiv I(\mathbf{r}) - I_D(\mathbf{r})$ as

$$\frac{\langle \delta I(\mathbf{r})\delta I(\mathbf{r}')\rangle}{I_D(\mathbf{r})I_D(\mathbf{r}')} = C_1(\mathbf{r},\mathbf{r}') + C_2(\mathbf{r},\mathbf{r}') + C_3(\mathbf{r},\mathbf{r}')\ . \tag{7}$$

The first contribution $C_1(\mathbf{r},\mathbf{r}') = \frac{2\pi l}{k^2}\delta(\mathbf{r}-\mathbf{r}')$ (see Eq.(S47)) is short ranged and independent of $g_{\mathcal{L}}$. The two other contributions are long ranged, and respectively proportional to $1/g_{\mathcal{L}}$ and $1/g_{\mathcal{L}}^2$. All three terms contribute to specific features of interference speckle patterns [19], and have been measured in weakly disordered electronic and photonic media [15, 20–24].

This $1/g_{\mathcal{L}}$ expansion can be obtained in a different but completely equivalent and elegant way by noting that quantum crossings occur at lengths of order $(lk^{-2})^{1/3}$, smaller than the elastic mean free path l. This allows to separate large scale ($\gg l$) incoherent diffusive physics from small scale, coherent and phase preserving quantum crossings. This partition is described by a Langevin equation,

$$\mathbf{j}(\mathbf{r}) = -D\boldsymbol{\nabla} I(\mathbf{r}) + \boldsymbol{\nu}(\boldsymbol{r}) \tag{8}$$

which extends the Fick's law, Eq.(4), to the fluctuating, i.e. non disorder averaged quantities $I(\mathbf{r}) \equiv I_D(\mathbf{r}) + \delta I(\mathbf{r})$ and $\mathbf{j}(\mathbf{r}) \equiv \mathbf{j_D}(\mathbf{r}) + \delta\mathbf{j}(\mathbf{r})$, by adding a zero average noise defined by the vector $\boldsymbol{\nu}(\boldsymbol{r})$. This picture, originally presented in [25], allows to reproduce the $1/g_{\mathcal{L}}$ expansion of Eq.(7) by systematically including quantum crossings contributions into $\boldsymbol{\nu}(\boldsymbol{r})$. To lowest order in $1/g_{\mathcal{L}}$ (SM section 3),

$$\langle \nu_\alpha(\mathbf{r})\nu_\beta(\mathbf{r}')\rangle = \delta_{\alpha\beta}\, c_0 I_D^2(\mathbf{r})\, \delta(\mathbf{r}-\mathbf{r}') \tag{9}$$

where $c_0 \equiv \frac{2\pi l v^2}{3k^2}$. We can rewrite the noise term under the form, $\boldsymbol{\nu}(\boldsymbol{r}) = \sqrt{\sigma}\,\boldsymbol{\eta}(\mathbf{r})$, where $\langle \eta_\alpha(\mathbf{r})\eta_\beta(\mathbf{r}')\rangle = \delta_{\alpha\beta}\,\delta(\mathbf{r}-\mathbf{r}')$ [26], with a strength,

$$\sigma = c_0\, I_D^2(\mathbf{r})\,, \tag{10}$$

which depends quadratically on the average diffusive radiation intensity $I_D(\mathbf{r})$ [27].

This effective Langevin description, based on the two parameters D and σ, provides a complete hydrodynamic description of the coherent light flow in the random medium. Moreover, it is appealing since its specific dependence upon a constant D and a quadratic σ, immediately draws a similarity with the Kipnis-Marchioro-Presutti (KMP) process – a heat transfer model for boundary driven one dimensional chains of mechanically uncoupled oscillators strongly out of equilibrium [28, 29], well described by the macroscopic fluctuation theory [30]. A correspondence with this process is obtained by formally identifying the radiation intensity I to the energy density, and $\mathbf{j}$ to the heat flow [31]. Despite this formal mapping, it is essential to note that the physical source of non equilibrium is very different in the two cases. While in the KMP model, energy density fluctuations result from thermal effects due to the coupling to two reservoirs at distinct temperatures, intensity fluctuations of the light flow result solely from the illumination of the random scattering medium.

A general Einstein relation exists which relates the parameters D and σ characteristic of the hydrodynamic regime of strongly non equilibrium systems. It is given by $\sigma = D\chi(\mathbf{r})$, where $\chi(\mathbf{r})$ is the static compressibility [29, 32]. For the coherent light flow,

$$\chi(\mathbf{r}) = \frac{c_0}{D} I_D^2(\mathbf{r})\,, \tag{11}$$

which from Eq.(10), satisfies the Einstein relation (SM section 4).

We are now in a position to calculate the radiation force $\mathbf{f}$, which includes, on top of its average $\langle\mathbf{f}\rangle$, a fluctuating (FIF) part $\boldsymbol{f} \equiv \mathbf{f} - \langle\mathbf{f}\rangle$ induced by intensity fluctuations. In the geometry of Fig.1, a dielectric plate, or membrane, of surface $S = L_\perp \times L_\parallel$, perpendicular to $\widehat{\mathbf{n}} = \widehat{\mathbf{z}}$, is inserted in the scattering medium so as to cancel by symmetry the average force $\langle\mathbf{f}\rangle$. The fluctuating part is readily obtained by substituting Eq.(8) into Eq.(3) together with Eq.(4) and it is given by

$$\begin{aligned}\langle \boldsymbol{f}^2\rangle &= \frac{1}{v^4}\iint\limits_{S\times S} d\mathbf{r}d\mathbf{r}'[D^2\partial_z\partial_{z'}\langle\delta I(\mathbf{r})\delta I(\mathbf{r}')\rangle + \langle\nu_z(\mathbf{r})\nu_{z'}(\mathbf{r}')\rangle] \\ &\equiv \sum_{j=1}^{3}\boldsymbol{f}_{\boldsymbol{j}}^2 + \boldsymbol{f}_{\boldsymbol{\nu}}^2\,,\end{aligned} \tag{12}$$

where $\boldsymbol{f}_{\boldsymbol{j}}^2$ is the counterpart of the corresponding term in Eq.(7) and $\boldsymbol{f}_{\boldsymbol{\nu}}^2$ results from the noise term. The contribution $\boldsymbol{f}_{\boldsymbol{1}}^2$ is always negligible compared to $\boldsymbol{f}_{\boldsymbol{\nu}}^2$, as can easily be seen by considering the corresponding fluctuating forces on the faces of a cubic L^3 geometry with $L \gg l$ and without inner plate. The expression of C_1 together with Eqs.(5,9), implies that $\boldsymbol{f}_{\boldsymbol{1}}^2 \sim \left(\frac{l}{L}\right)^2 \boldsymbol{f}_{\boldsymbol{\nu}}^2$, hence $\boldsymbol{f}_{\boldsymbol{1}}^2$ is negligible. The term $\boldsymbol{f}_{\boldsymbol{3}}^2$ induced by C_3 is of order $1/g_{\mathcal{L}}^2$ and therefore also negligible. Finally, the behaviour of $\boldsymbol{f}_{\boldsymbol{\nu}}^2$ is readily obtained from Eqs.(5,9,11), namely $\boldsymbol{f}_{\boldsymbol{\nu}}^2 = \frac{D}{v^4}\iint\limits_{S\times S} d\mathbf{r}d\mathbf{r}'\chi(\mathbf{r})\delta(\mathbf{r}-\mathbf{r}') = \frac{1}{g_{\mathcal{L}}}\frac{\mathcal{P}^2}{v^2}\mathcal{Q}_\nu$, where $\mathcal{Q}_\nu$ is a dimensionless number characteristic of the system geometry. Then, as can be anticipated from Eq.(7), $\boldsymbol{f}_{\boldsymbol{2}}^2$ behaves like $1/g_{\mathcal{L}}$ and it is proportional to $\boldsymbol{f}_{\boldsymbol{\nu}}^2$ (SM section 5.1), so that finally the fluctuating force has the general form Eq.(1) presented in the introductory paragraph.

We now evaluate more quantitatively the amplitude of the FIF in Eq.(1). Their dependence on the geometry and boundary conditions allows for a wide choice of parameters for control and amplification. Indeed, boundary conditions play an essential role in the determination of the dimensionless $\mathcal{Q}$'s, and even enable to measure independently $\boldsymbol{f}_2$ or $\boldsymbol{f}_{\boldsymbol{\nu}}$ in Eq.(12) (SM section 5.2). We highlight that a measurement of the sole contribution $\boldsymbol{f}_{\boldsymbol{\nu}}$ of the noise induced by coherent effects, a by-product of our approach, cannot be achieved with other physical quantities, e.g. the transmission coefficient. Here, considering in the geometry of Fig.1, an absorbing plate where $I_D(\mathbf{r}) = 0$ (Fig.2.a), selects only $\boldsymbol{f}_2$ which contributes with a maximum for an optimal value of L_1. Alternatively, inserting a reflective plate with $\partial_z I_D(\mathbf{r}) = 0$ selects $\boldsymbol{f}_{\boldsymbol{\nu}}$ and leads to FIF with a power law dependence with L_1 (see Fig.2.b and SM section 5.2).

Sizeable efforts have been devoted to the development of high sensitivity cantilevers able to measure forces of weak amplitude [33]. We propose to observe mesoscopic FIF using an atomic force microscope, in a setup similar to [10] where Casimir-Lifshitz forces of a few piconewtons have been measured between a gold plate and a gold coated sphere immersed in a liquid. Replacing the liquid by a weakly scattering medium $kl \sim 10$ and using square plates of size $40\,\mu\text{m}\times 40\,\mu\text{m}$ – the typical size of the sphere used in [10] – and illuminating the medium with a light

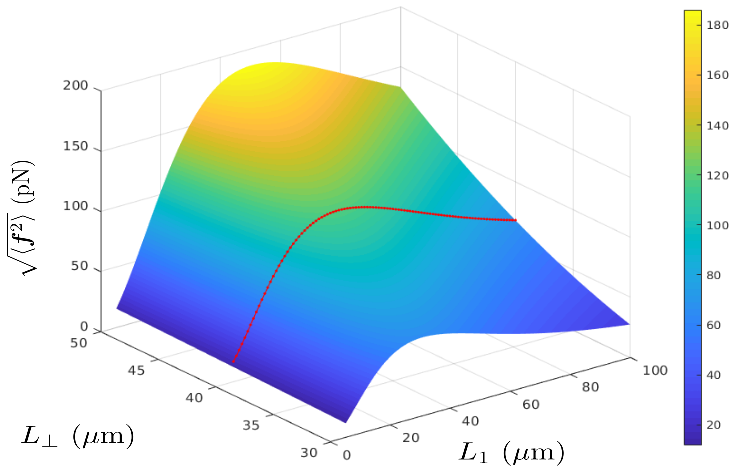

(a)

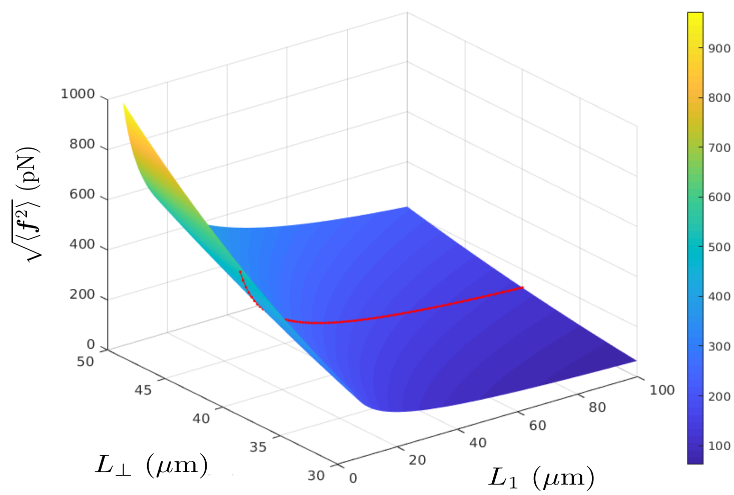

(b)

FIG. 2. Amplitude of $\sqrt{\langle \boldsymbol{f}^2 \rangle}$ on the plate in Fig.1 as a function of L_1 and $L_\perp$ with fixed $L_\parallel = 40\,\mu$m and $l = 1\,\mu$m. **(a)** Absorbing plate with $I_D(\mathbf{r}) = 0$, so that $\langle \boldsymbol{f}^2 \rangle = \boldsymbol{f}_2^2$. It vanishes in both limits $L_1 \to 0$ and $L_1 \to +\infty$, which results from the form of $I_D(\mathbf{r}) I_D(\mathbf{r}') C_2(\mathbf{r}, \mathbf{r}')$ (see SM section 5.1 and 5.2). **(b)** Reflecting plate where $\partial_z I_D(\mathbf{r}) = 0$, hence $\boldsymbol{f}_2 = 0$ and $\langle \boldsymbol{f}^2 \rangle = \boldsymbol{f}_\nu^2$. From Eq.(9) and Eq.(12), it appears that $\boldsymbol{f}_\nu^2$ scales like $1/\sqrt{L_1}$ (see SM section 5.2). The red lines correspond to $L_\perp = 40\,\mu$m as in Table I.

beam of intensity $I \sim 10^9\,\mathrm{W} \cdot m^{-2}$, we expect light FIF of amplitude up to a few hundreds of piconewtons, i.e. strong enough to be detected. These results are summarized in Table I.

Eq.(1), together with the hydrodynamic description of coherent effects based on the Langevin equation (8), constitute the main results of this paper. Let us now discuss the scope of our findings in the context of ongoing research in mesoscopic physics and statistical mechanics, as well as applications. Aspects of diffusive light propagation, either incoherent or coherent, have already been thoroughly studied in the literature. For electronic quantum waves, the focus is mainly on transport properties, better accessible in mesoscopic devices and which stand as a favorite candidate to observe the elusive Anderson localization transition for large enough disorder. For radiation and other classical waves, transmission properties and long range correlations either spatial or spectral, have been also extensively studied. Despite these thorough investigations, mechanical effects resulting from coherent mesoscopic effects of diffusive light as presented here, have never been envisaged. They open a new and alternative approach to the field. From a fundamental viewpoint, the existence of fluctuation induced forces easily and solely monitored by the dimensionless conductance Eq.(6) has a threefold interest. First, the analogy here unveiled, between long range induced forces in a coherent mesoscopic light flow and in non equilibrium systems, should arouse experimental attention to observe such forces in the realm of radiation flow in Casimir physics. Second, coherent mechanical forces are sensitive to the disorder strength through the conductance $g_\mathcal{L}$. Hence, albeit non transport quantities, these forces can be used as a new effective probe to study the existence and criticality of Anderson localization transition both theoretically and experimentally. Third, potential applications of mechanical forces induced by a coherent diffusive radiation flow are diverse and promising: in addition to transmission measurements extensively used, they provide a new type of mechanical and sensitive sensors at submicronic scale rather easy to implement and useful in soft condensed matter, biophysics [34], nanoelectrome-

TABLE I. Typical strength of light FIF in the setup of Fig.1 obtained for visible light, $k \sim 10^7\ \mathrm{m}^{-1}$ and an elastic mean free path $l \simeq 1\,\mu$m i.e in a weakly disordered medium ($kl \sim 10$) and $v = 2.10^8\ \mathrm{m}\cdot\mathrm{s}^{-1}$. We consider the optimal case of reflecting cavity edges along $\hat{\mathbf{x}}$ and absorbing edges along $\hat{\mathbf{y}}$ (see text) and compare the cases of an absorbing and reflecting plate (Fig.2). We obtain $g_\mathcal{L} = \frac{k^2 l}{3\pi} \frac{L_1 L_\perp L_\parallel}{\max(L_1^2, L_\perp^2, L_\parallel^2)}$ hence identifying the length $\mathcal{L}$ (see SM section 5.2). The amplitude of $\langle \boldsymbol{f}^2 \rangle$ is calculated for different values of L_1 ranging from $5\,\mu$m to $100\,\mu$m, with $L_\perp = L_\parallel = 40\,\mu$m, so that $L_1 > l$ and $g_\mathcal{L} \gg 1$ in all cases. We choose $I = 10^9\ \mathrm{W}\cdot\mathrm{m}^{-2}$, an intensity strong enough to obtain measurable forces without altering the medium.

	$L_1(\mu\mathrm{m})$	$\sqrt{\langle \boldsymbol{f}^2 \rangle}$(pN)	$\mathcal{Q}_2 + \mathcal{Q}_\nu$	$g_\mathcal{L}$
Absorbing plate $\mathcal{Q}_\nu = 0$	5	13	$1.0 \cdot 10^{-3}$	53
	40	118	$1.0 \cdot 10^{-2}$	424
	100	68	$2.2 \cdot 10^{-4}$	170
Reflecting plate $\mathcal{Q}_2 = 0$	5	567	1.9	53
	40	201	$2.3 \cdot 10^{-2}$	424
	100	127	$7.6 \cdot 10^{-4}$	170

chanical (NEMS) and quantum technologies [35, 36]. Finally, we wish to highlight that the mapping we have presented between coherent light flow and out of equilibrium hydrodynamics is easily generalisable to other quantum or classical mesoscopic effects, e.g in nanoelectronics and superconductivity [37]. A clear asset of this type of approach is in its dependence upon two parameters only, thus making it a candidate to efficient machine learning algorithms.

This work was supported by the Israel Science Foundation Grant No. 924/09. We are grateful to Ohad Shpielberg for discussions, Boris Timchenko, Marc Soret and Igor Khmelnitsky for a critical reading of the manuscript and Yaroslav Don for his help in the preparation of the manuscript.

* eric@physics.technion.ac.il

[1] M. Kardar, R. Golestanian, "The Friction of Vacuum, and other Fluctuation-Induced Forces," Rev. Mod. Phys. **71**, (1999).
[2] H. B. G. Casimir, "On the attraction between two perfectly conducting plates," Proc. Kon. Ned. Akad. Wet. **B51**, 793–795 (1948).
[3] M. E. Fisher, P.-G. de Gennes, "Phénomènes aux parois dans un mélange binaire critique," C. R. Acad. Sci. Paris **287**, (1978).
[4] A. Aminov, Y. Kafri, M. Kardar, "Fluctuation-Induced Forces in Nonequilibrium Diffusive Dynamics," Phys. Rev. Lett. **114**, 230602 (2015).
[5] T. R. Kirkpatrick, J. M. Ortiz de Zárate, J. V. Sengers, "Fluctuation-induced pressures in fluids in thermal nonequilibrium steady states," Phys. Rev. E **89**, 022145 (2014).
[6] D. S. Dean, B.-S. Lu, A. C. Maggs, R. Podgornik, "Nonequilibrium Tuning of the Thermal Casimir Effect," Phys. Rev. Lett. **116**, (2016).
[7] R. Messina, D. A. R. Dalvit, P. A. Maia Neto, A. Lambrecht and S. Reynaud, "Dispersive interactions between atoms and nonplanar surfaces," Phys. Rev. A **80**, 022119 (2009).
[8] S. K. Lamoreaux, "Demonstration of the Casimir Force in the 0.6 to 6 μm Range," Phys. Rev. Lett. **78**, (1997).
[9] A. Lambrecht, S. Reynaud, "Casimir force between metallic mirrors," Eur. Phys. J. B **8**, 309 (2000).
[10] J. N. Munday, F. Capasso, V. A. Parsegian, "Measured long-range repulsive Casimir-Lifshitz forces," Nat. Letters. **457**, 170–173 (2009).
[11] G. Jourdan and A. Lambrecht and F. Comin and J. Chevrier, "Quantitative non-contact dynamic Casimir force measurements," Europhys. Lett. **85**, 31001 (2009).
[12] U. Mohideen and A. Roy, "Precision Measurement of the Casimir Force from 0.1 to 0.9 m," Phys. Rev. Lett. **81**, 4549 (1998).
[13] C. Hertlein, L. Helden, A. Gambassi, S. Dietrich, C. Bechinger, "Direct measurement of critical Casimir forces," Nature **451**, 172 (2008).
[14] Polarization effects are usually decoupled from disorder. For more elaborations, see [15].
[15] E. Akkermans, G. Montambaux, *Mesoscopic physics of electrons and photons* (Cambridge University Press, 2007).
[16] A. Ishimaru, *Wave propagation and scattering in random media* (Academic Press, 1978).
[17] This phenomenological picture for coherent mesoscopic effects is presented at an introductory level in [15], section 1.7.
[18] See chapter 12 in [15].
[19] J. W. Goodman, *Statistical Optics* (Wiley Classics Library Edition, 2000).
[20] M. Kaveh, M. Rosenbluh, I. Freund, "Speckle patterns permit direct observation of phase breaking," Nature **326**, 778–780 (1987).
[21] F. Scheffold, G. Maret, "Universal Conductance Fluctuations of Light," Phys. Rev. Lett. **81**, 5800 (1998).
[22] F. Scheffold, W. Hartl, G. Maret, E. Matijevic, "Observation of long-range correlations in temporal intensity fluctuations of light," Phys. Rev. B **56**, 10942 (1997).
[23] J. F. de Boer, M. P. van Albada, A. Lagendijk, "Transmission and intensity correlations in wave propagation through random media," Phys. Rev. B **45**, 658 (1992).
[24] M. J. Stephen, G. Cwilich, "Intensity correlation functions and fluctuations in light scattered from a random medium," Phys. Rev. Lett. **59**, 285 (1987).
[25] B. Z. Spivak, A. Yu. Zjuzin, "Langevin description of mesoscopic fluctuations in random medium," Sov. Phys. JETP **93**, 994–1006 (1987).
[26] The gaussian noise assumption in Eq.(9) is justified since the FIF do not depend on higher moments.
[27] The Langevin approach is valid for a weak noise, i.e. when σ goes to zero with the system size. This requirement is here satisfied, see SM section 4.
[28] C. Kipnis, C. Marchioro, E. Presutti, "Heat Flow in an Exactly Solvable Model," J. Stat. Phys. **27**, 65 (1982).
[29] L. Bertini, D. Gabrielli, J. L. Lebowitz, "Large Deviations for a Stochastic Model of Heat Flow," J. Stat. Phys. **121**, (2005).
[30] L. Bertini, A. De Sole, D. Gabrielli et al., "Macroscopic fluctuation theory," Rev. Mod. Phys. **87**, 593 (2015).
[31] The Langevin equation (8) is time-independent, so that the correspondence is obtained by integrating the KMP Langevin equation over short time scales up to the elastic mean free time $\tau = l/c$ (see SM section 4).
[32] H. Spohn, *Large Scale Dynamics of Interacting Particles* (Springer, Berlin, 1991).
[33] D. Yan R. Castillo-Garza, C.-C. Chang and U. Mohideen, "Customized silicon cantilevers for Casimir force experiments using focused ion beam milling," J. Phys. Conf. Ser. **161**, 012005 (2009).
[34] K. Bradonjić, J. D. Swain, A. Widom, Y. N. Srivastava, "The Casimir Effect in Biology: The Role of Molecular Quantum Electrodynamics in Linear Aggregations of Red Blood Cells," J. Phys.: Conf. Ser **161**, (2009).
[35] T. J. Kippenberg and K. J. Vahala, "Cavity Opto-Mechanics," Opt. Express **15**, 17172 (2007).
[36] O. Arcizet, P.-F. Cohadon, T. Briant, M. Pinard, A. Heidmann, "Radiation-pressure cooling and optomechanical instability of a micromirror," Nature **444**, 71 (2006).
[37] L. Henriet, A. N. Jordan and K. Le Hur, "Electrical current from quantum vacuum fluctuations in nanoengines," Phys. Rev. B **92**, 125306 (2015).